(12) J. O. Edwards, G. C. Morrison, V. F. Ross, and J. W. Schulz, *J. Am. Chem. Soc.*, 77, 266 (1955).
(13) F. C. Kracek, G. W. Morey, and H. E. Merwin, *Am. J. Sci.*, 143 (1938).
(14) S. Pawlenko, *Z. Anorg. Allg. Chem.*, **315**, 147 (1962).
(15) C. R. Peters and M. E. Milberg, *Acta Crystallogr*, **17**, 229 (1964).
(16) M. Marezio, H. A. Plettinger, and W. H. Zachariasen, *Acta Crystallogr.*, **16**, 594 (1963).
(17) J. Goubeau and H. Keller, *Z. Anorg. Allg. Chem.*, **272**, 303 (1953).
(18) J. L. Parsons, *J. Chem. Phys.*, **33**, 1860 (1960).
(19) W. H. Zachariasen, *Acta Crystallogr.*, **16**, 385 (1963).
(20) R. K. Momii and N. H. Nachtrieb, *Inorg. Chem.*, **6**, 1189 (1967).
(21) H. D. Smith, Jr., and R. J. Wiersema, *Inorg. Chem.*, **11**, 1152 (1972).
(22) P. J. Bray and J. G. O'Keefe, *Phys. Chem. Glasses*, **4**, 37 (1963).
(23) R. E. Mesmer and A. C. Rutenberg, *Inorg. Chem.*, **12**, 699 (1973).

Contribution from the Department of Chemistry,
University of Pittsburgh, Pittsburgh, Pennsylvania 15260

Solubility of Hydrogen in Intermetallics Containing Rare Earth and 3d Transition Metals

C. A. BECHMAN, A. GOUDY, T. TAKESHITA, W. E. WALLACE,* and R. S. CRAIG

Received November 5, 1975 AIC50795C

Pressure–composition isotherms have been determined for the systems RCo_3–H and RFe_3–H, with R = Gd, Tb, Dy, and Ho, and also for $ErFe_3$–H. The studies show certain systematics in regard to the affinity of the alloy for hydrogen: (1) it is greater for the Fe compounds than for the corresponding Co compounds; (2) it decreases as the atomic number of R increases; (3) it increases with increased rare earth content of the compound. The systematic trends are thought to be brought on by systematic variations in the band structure produced by variations in composition and stoichiometry. The hydrogen storage capacities of the RT_3 phases (T = Fe or Co) exceed those of the RCo_5 phases and the well-known hydrogen absorber $LaNi_5$. The amount of hydrogen stored at pressures of 400 psi ranges from about 4 to 6 × 10^{22} atoms/cm^3; some of these exceed the particle density of liquid hydrogen, 4.2 × 10^{22} atoms/cm^3.

Introduction

A number of RT_5 compounds[1-3] (R is a rare earth and T is Co or Ni) have been found to absorb and desorb rapidly relatively large quantities of hydrogen, some under moderate pressures and at room temperature. Buschow and Van Mal[4] have shown that a shift in the stoichiometry of $LaNi_5$ in the nickel-poor direction results in an increase in the quantity of hydrogen absorbed by the material at a reduced pressure. Structurally, RT_3 compounds may be considered[5] to be T-deficient RT_5 phases; hence, it is of considerable interest to examine these materials as hydrogen absorbers for comparison with the RT_5 phases and the T-deficient RT_5 phases.

In a previous communication we reported hydrogen absorption data for $ErCo_3$ and some information for the $DyCo_3$–H and $HoCo_3$–H systems.[3] This study has been extended in the present work to include $TbCo_3$ and $GdCo_3$ and also the corresponding RFe_3 series. Additional results for the Dy- and Ho-containing ternaries are also presented.

In the comprehensive study of the RCo_5 series as H_2 absorbers carried out by Kuijpers,[6] a systematic trend was noted: the hydrogen vapor pressure measured at a given temperature and at a fixed H:RCo_5 ratio increased with increasing atomic number of R, indicating a decreasing affinity for hydrogen as the atomic number of R is increased. The lanthanide contraction is operative in the RCo_5 sequence so that the observation of Kuijpers is equivalent to a correlation between affinity for H_2 and the size of the RCo_2 unit cell. In the phase based on the composition $LaNi_5$ the volume of the unit cell decreases as the sample departs from ideal stoichiometry in the nickel-rich direction. The results of Buschow and Van Mal[4] referred to above also show a direct relationship between affinity of the metal for H_2 and the size of the unit cell. The RFe_3 phase has larger unit cell dimensions than the corresponding RCo_3; therefore, if the systematics observed by Kuijpers and by Buschow and Van Mal hold, it might be expected that the affinity for H_2 would be in the order RFe_3 > RCo_3. To ascertain whether this was indeed the case was one of the motivations for the present study. In addition, we were interested in the general behavior of these two series of materials as solvents for H_2 and also in any other systematic characteristics that they might exhibit which would shed light on the truly extraordinary features of the RT_x systems—their ability to contain large amounts of hydrogen and the great rapidity with which they absorb and release hydrogen.

Experimental Section

Samples were prepared by induction melting the constituent metals in a water-cooled copper boat under a purified argon atmosphere. The metals used were the highest purity materials commercially available: cobalt >99.999%, iron >99.999% and rare earths >99.9%, exclusive of gaseous impurities. After melting, the samples were annealed and homogenized in the cold boat so that no additional phases could be detected when subjected to x-ray analysis. The hydriding system was constructed of stainless steel. The temperature of the sample was controlled by a stirred water bath below 100 °C and by an electric furnace above that temperature. The water bath was controlled to within 0.1 °C and the furnace to within 0.25 °C.

The samples were crushed to less than 1-mm particle size in air before being placed in the sample holder. They were then activated by allowing them to sequentially absorb and desorb hydrogen until the quantity of hydrogen absorbed became constant. The absorption process was conducted at pressures up to 1500 psig and was usually complete after about 2 min; however, at least 2 h was allowed for the system to reach equilibrium since this step is strongly exothermic. The desorption was accomplished by allowing the hydrogen to flow out through water into an inverted buret to atmospheric pressure, followed by pumping on the sample with a mechanical pump. During the final stage of pumping the temperature of the sample was increased to about 250 °C.

Desorption pressure–composition isotherms were determined by first measuring in a known quantity of H_2 and then removing measured quantities of hydrogen from the system and establishing the resulting pressure at equilibrium. The dead spaces in the hydriding system had been calibrated and appropriate allowance was made for H_2 remaining in the dead spaces. Time to reach equilibrium varied from 0.5 to 2 h above atmospheric pressure but up to 12 h below. Absorption pressure–composition isotherms were established by metering in fixed amounts of H_2 and waiting for the pressure to become constant between additions. Allowance was again made for the dead space H_2. Ashcroft test gauges were used for pressure measurements above

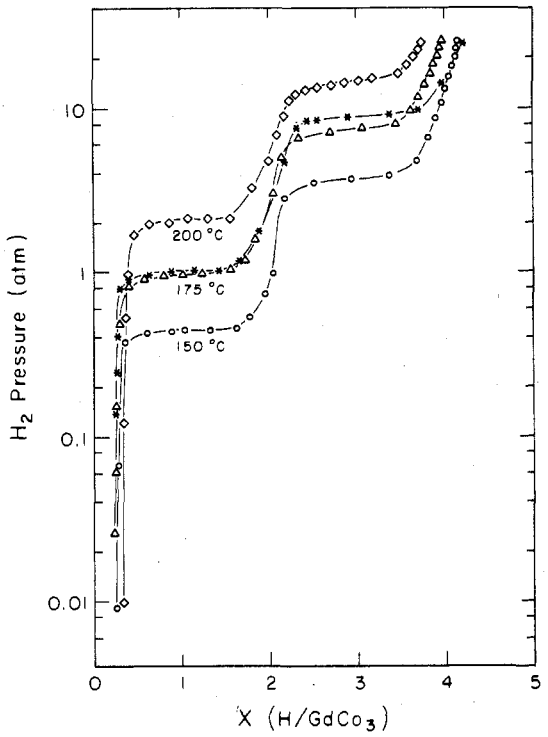

Figure 1. Pressure-composition isotherms for the $GdCo_3$-H_2 system.

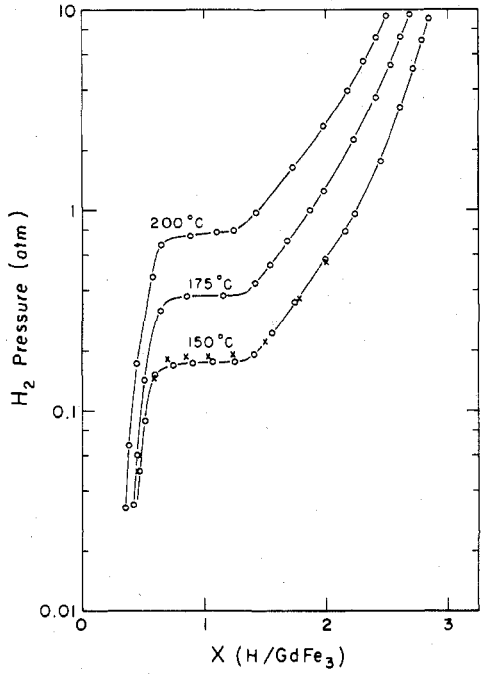

Figure 2. Pressure-composition isotherms for the $GdFe_3$-H_2 system.

atmospheric pressure. Either a Texas Instrument fused quartz precision gauge or a U-tube manometer was used for pressures below 1 atm.

Results and Discussion

Pressure–composition isotherms for the $GdCo_3$–H_2 system, which are similar to those of the other cobalt compounds, are given in Figure 1. Pressure–composition isotherms for the $GdFe_3$–H_2 system, which are typical of all the RFe_3 compounds, are shown in Figure 2. The curves marked with asterisks and crosses in Figures 1 and 2, respectively, correspond to data taken during the absorption process described above. The other curves were determined by the desorption process. Pertinent data for the other 1:3 compounds are summarized in Table I. The maximum hydrogen solubilities at 400 psig are shown in Table II.

Table I. Plateau Pressure as a Function of Temperature[a]

Compd	Temp, °C	Plateau presure, atm α–β	Plateau presure, atm β–γ
$GdCo_3H_x$	150	0.44	3.69
	175	0.97	7.40
	200	2.05	14.26
$TbCo_3H_x$	100	0.18	1.54
	125	0.47	3.88
	150	1.13	8.35
$DyCo_3H_x$	101	*b*	3.00
	124	*b*	6.40
$HoCo_3H_x$	86	*b*	2.90
	101	*b*	5.10
$ErCo_3H_x$	51	*b*	1.65
	59	*b*	2.10
	75	*b*	4.40
	101	1.50	10.20
$GdFe_3H_x$	150		0.18[c]
	175		0.37
	200		0.78
$TbFe_3H_x$	125		0.13
	150		0.23
	200		1.15
$DyFe_3H_x$	125		0.16
	150		0.38
	200		1.58
$HoFe_3H_x$	125		0.28
	150		0.63
	200		2.42
$ErFe_3H_x$	125		0.53
	150		1.15
	200		4.20

[a] As is seen in Figures 1 and 2 the pressure is not independent of composition in the two-phase region. Instead there is a small positive slope to the curve. The plateau pressure is taken as that pressure corresponding to the composition midway along the composition range over which pressure is weakly dependent on composition. [b] These materials were studied in the earlier investigation.[3] The plateau pressures for the α–β transition were less than 1 atm and were not determined quantitatively. [c] The results for the RFe_3 compounds apply to the α–γ transition (see text).

Table II. H_2 Solubility at 400 psig (28.2 atm) and 125 °C[a]

Compd	H:RT_3	Compd	H:RT_3
$GdCo_3$	4.3	$GdFe_3$	3.2
$TbCo_3$	4.1	$TbFe_3$	3.6
$DyCo_3$	4.1	$DyFe_3$	3.2
$HoCo_3$	4.0	$HoFe_3$	3.2
$ErCo_3$	4.0	$ErFe_3$	2.8

[a] The H_2 uptake increases slowly as pressure is raised above 400 psig. For example, with $GdCo_3$ the composition achieved at 1500 psig and 125 °C is $GdCo_3H_{4.6}$. The limiting composition for 2–3000 psig appears to be approximately $GdCo_3H_5$.

Over the pressure ranges studied two plateau regions were found for the 1:3 cobalt compounds but only one for the 1:3 iron phases. These data indicate the existence of three and two crystallographically distinguishable hydrides in the 1:3 Co- and Fe-containing systems, respectively. In the discussion which follows we designate the three hydrides α, β, and γ. α is the terminal phase based upon RCo_3 or RFe_3 and γ is the most H-rich phase in the RCo_3 system. The heats of reaction for the transitions were obtained from plots of the van't Hoff isochores for these two-phase regions.

Complete isotherms were determined during both absorption and desorption for the compounds $HoFe_3$ and $DyFe_3$. In the case of $HoFe_3$, the ΔH values obtained from absorption data were about 2% smaller than those obtained from desorption data. In the case of $DyFe_3$ the difference was about 4%.

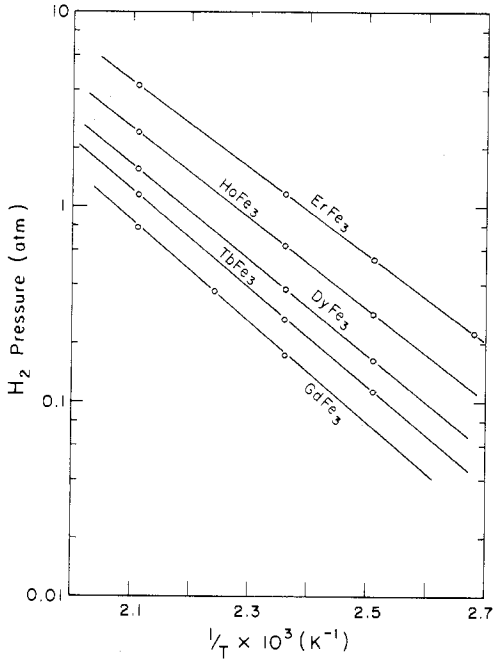

Figure 3. Pressure of H_2 vs. $1/T$ (semilog plot) for the RFe_3-H_2 system.

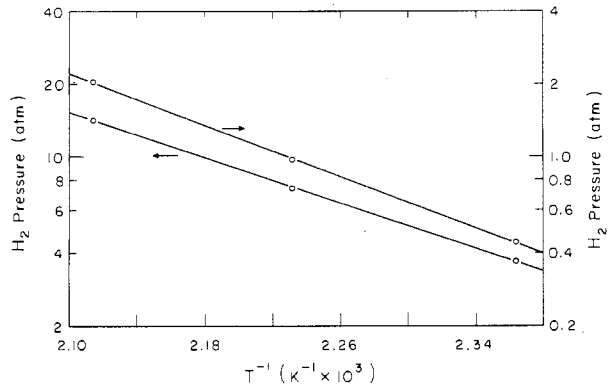

Figure 4. Pressure of H_2 vs. $1/T$ (semilog plot) for the $GdCo_3$-H_2 system. The two straight lines correspond to the two plateaus shown in Figure 1.

Table III. Heats of Transition (kcal/mol of H_2)

System	α-β plateau	β-α plateau	α-γ plateau	Temp range, °C
$GdCo_3$-H_2	12.2	10.7		150-200
$TbCo_3$-H_2	11.6	10.6		100-150
$DyCo_3$-H_2		10.1		100-125
$HoCo_3$-H_2		9.2		85-100
$ErCo_3$-H_2		9.2		50-100
$GdFe_3$-H_2			12.1	150-200
$TbFe_3$-H_2			11.5	125-200
$DyFe_3$-H_2			11.3	125-200
$HoFe_3$-H_2			10.7	125-200
$ErFe_3$-H_2			10.3	125-200

Complete sets of absorption isotherms were not obtained for other RFe_3 compounds. Our observations showed that hysteresis is small in these systems, and we assume that the differences in the other ΔH values for absorption and desorption will be similar in magnitude. Typical plots are given in Figures 3 and 4. Values obtained for the other 1:3 phases are summarized in Table III.

Diffraction patterns of the hydrogenated materials were obtained to confirm that the sample had not decomposed and to determine the effect of the dissolved hydrogen on the lattice dimensions. These were obtained utilizing a Picker 6148 diffractometer with Cu Kα radiation. The diffraction lines were usually rather sharp. Lattice parameters were obtained by the use of an iterative least-squares program. Results obtained are presented in Table IV.

Table IV. Lattice Parameters of Parent Metals and Hydrides and Hydrogen Particle Densities

Compd	a, Å	c, Å	c/a	ΔV, %	ΔV/H atom	(H atoms/cm^3 of hydride) $\times 10^{-22}$
$GdCo_3$	5.038	24.66	4.894			
$GdCo_3H_{2.2}$	5.023	27.31	5.438	10.1	2.8	3.3
$GdCo_3H_{4.6}$	5.314	27.14	5.107	22.5	2.9	6.2
$TbCo_3$	5.023	24.50	4.878			
$TbCo_3H_{1.8}$	5.010	26.74	5.337	8.6	2.8	2.6
$TbCo_3H_{4.5}$	5.255	26.84	5.107	19.9	2.6	6.3
$DyCo_3$	4.987	24.36	4.885			
$DyCo_3H_{2.0}$	4.999	26.28	5.257	8.4	2.4	3.2
$DyCo_3H_{4.3}$	5.224	26.37	5.048	18.8	2.6	6.2
$HoCo_3$	4.981	24.30	4.878			
$HoCo_3H_{1.9}$	4.991	26.17	5.243	8.1	2.5	3.0
$HoCo_3H_{4.2}$	5.250	26.32	5.013	20.3	2.8	6.0
$ErCo_3$	4.979	24.28	4.876			
$ErCo_3H_{1.9}$	4.995	25.96	5.197	7.6	2.3	3.1
$ErCo_3H_{4.2}$	5.217	26.03	4.989	17.7	2.4	6.2
$GdFe_3$	5.167	24.71	4.782			
$GdFe_3H_{3.1}$	5.387	27.01	5.014	17.5	3.8	4.1
$TbFe_3$	5.143	24.64	4.790			
$TbFe_3H_{4.2}$	5.355	26.71	4.987	17.5	2.6	5.6
$DyFe_3$	5.130	24.52	4.779			
$DyFe_3H_{3.0}$	5.310	26.59	5.008	16.2	3.3	4.2
$HoFe_3$	5.117	24.48	4.784			
$HoFe_3H_{3.6}$	5.316	26.39	4.964	16.4	2.8	5.0
$ErFe_3$	5.104	24.56	4.812			
$ErFe_3H_{2.7}$	5.267	26.16	4.967	13.4	3.0	3.9

Table V. Particle Density of Hydrogen in Several Materials

Compd	(No. of H atoms/cm^3) $\times 10^{-22}$	Compd	(No. of H atoms/cm^3) $\times 10^{-22}$
$GdCo_3H_{4.6}$	6.2	$LaNi_5H_{5.9}$	5.5
$ErCo_3H_{4.2}$	6.2	$PrCo_5H_{2.8}$	3.0
$TbFe_3H_{4.2}$	5.6	Liq hydrogen	4.2
$ErFe_3H_{2.7}$	3.9		

Hydrides of the RCo_3 series were found to be more stable, in the sense of reduced H_2 escaping tendency and absorbing more hydrogen per unit volume, than the RCo_5 compounds studied by Kuijpers.[6] Thus, if the RCo_3 phases are regarded as Co-deficient RCo_5 phases, the expected behavior referred to in the first paragraph of the Introduction is confirmed. The pressure–composition data suggest a limiting composition of RCo_3H_5, whereas RCo_5H_4 is found for the RCo_5 hydride phases. The hydrogen absorption capacity of the 1:3 cobalt compounds is compared with that of $PrCo_5$, which typifies the RCo_5 phases, with that of $LaNi_5$, and with that of liquid hydrogen in Table V. The compositions shown in the table correspond to those which exist under conditions employed in these experiments, i.e., $P < 1000$ psi and $T < 200$ °C.

The RCo_3–H and RCo_5–H systems are similar in that both show the existence of three hydrides. In other respects they differ: when the RCo_5 phases are hydrided, the symmetry is degraded from hexagonal to orthorhombic, whereas the RCo_3 compounds are rhombohedral and their hydrides can also be indexed rhombohedrally. Moreover, in the case of the RCo_5 hydrides the expansion is in the basal plane with no appreciable change occurring in the c direction.[6] This is true even for the γ hydride. For the 1:3 compounds the formation of the β hydride results in an expansion in the c direction with no appreciable change in the a parameter. Upon formation of

the γ hydride, however, expansion takes place mainly in the a parameter. Interpretation of these interesting structural differences must await neutron diffraction measurements on the RCo_3 hydrides.

As noted above, the RFe_3 compounds form only two hydrides—the α or terminal phases and a second hydride. It is not entirely clear whether this should be designated β or γ. We incline to regard it as the γ hydride, by analogy with the crystallographic behavior of the RCo_3–H systems, since it involves an expansion in both the a and c parameters.

The H_2 pressures over the RFe_3–H systems are consistently lower than those of the RCo_3–H system in the two-phase regions. However, the RFe_3 phase absorbs less hydrogen at the maximum pressure utilized (400 psig) than the corresponding RCo_3 compound. Clearly, the γ RFe_3–H phase is stabler against hydrogen loss than the γ RCo_3–H phase at the hydrogen-poor end of the range of stability of the phase, and this order of stability exists for all hydrogen concentrations in the α phases.

There are then three classes of systematic behavior exhibited by the RT_x–H systems with regard to affinity for hydrogen: 1, a decrease as the atomic number of R increases; 2, a decrease as x increases; 3, a decrease when Fe is replaced by Co. In each of these three cases the decrease in affinity for hydrogen accompanies a change in chemical composition of stoichiometry which leads to a decrease in lattice size. We shall return to this point below.

Several absorption experiments were made to investigate the extent of the hysteresis between absorption and desorption of hydrogen for the 1:3 compounds. The behavior was found to be similar to that of the 1:5 cobalt compounds[7] in that the quantity $\Delta P/P$ at different temperatures for the same hydride was essentially constant. ΔP is the difference in plateau pressure observed in the absorption and desorption experiments. In most treatments of the hysteresis phenomenon the lattice expansion and the degree of hysteresis are interrelated.[8] In the 1:3 cobalt case where two hydrides are formed, the value of $\Delta P/P$ was greater for the γ hydride than for the β hydride. This is as expected since the lattice expansion is greater for the γ hydride.

The main difference in hydrogen absorption of the 1:3 cobalt or iron phases and that of the RT_5 compounds is the temperature at which desorption of hydrogen takes place above atmospheric pressure. The $LaNi_5$ desorption pressure at room temperature is 2.5 atm. For $LaCo_5$ a temperature of 90 °C is required to generate a hydrogen pressure exceeding 1 atm. The corresponding temperatures are 180 and 215 °C for the RCo_3 and RFe_3 phases, respectively. The RT_3 compounds thus afford a low-pressure hydrogen storage and delivery system which can easily be controlled by temperature.

Above, it was pointed out that in the RT_x phase the affinity for hydrogen is reduced by increasing the atomic number of R or T or by increasing x; all of these result in a more compact lattice. The work of Kuijpers and Loopstra[9] shows that molecular H_2 (or more exactly D_2) in $PrCo_5$ is broken down into the monatomic form and the atoms reside in certain interstitial sites. As the lattice size is diminished, the volume of the interstitial site decreases correspondingly. Superficially one might ascribe the systematics noted to the varying size of the site in which the H is occupied. We doubt that matters are that simple since the size of H^+, the species which probably most nearly resembles the dissolved form of hydrogen, is far smaller than that of the interstice. Probably the variations noted affect the band structure in these materials in a systematic way, and it is this which leads to the observed systematic trends noted in the hydrogen affinity of the RT_x phases. APW band calculations on selected RT_x phases are being carried out in this laboratory, and these may in time be useful in elucidating the receptivity of these phases for hydrogen.

Acknowledgment. This work was assisted by a contract with the Energy Research and Development Administration.

Registry No. $GdCo_3$, 12017-50-4; $TbCo_3$, 12187-47-2; $DyCo_3$, 12187-40-5; $HoCo_3$, 12140-00-0; $ErCo_3$, 12134-04-2; $GdFe_3$, 12023-46-0; $TbFe_3$, 12268-62-1; $DyFe_3$, 12517-72-5; $HoFe_3$, 12361-81-8; $ErFe_3$, 12400-78-1; H_2, 1333-74-0.

References and Notes

(1) J. H. N. van Vucht, F. A. Kuijpers, and H. C. A. M. Bruning, *Philips Res. Rep.*, **25**, 133 (1970).
(2) F. A. Kuijpers, *J. Less-Common Met.*, **27**, 27 (1972).
(3) T. Takeshita, W. E. Wallace, and R. S. Craig, *Inorg. Chem.*, **13**, 2282, 2283 (1974).
(4) K. H. J. Buschow and H. V. Van Mal, *J. Less-Common Met.*, **29**, 203 (1972).
(5) R. Lemaire and D. Paccard, *Bull. Soc. Fr. Mineral. Cristallogr.*, **92**, 9 (1969).
(6) F. A. Kuijpers, Ph.D. Thesis, Technische Hogeschool, Delft, 1973.
(7) F. A. Kuijpers and H. H. Van Mal, *J. Less-Common Met.*, **23**, 395 (1971).
(8) See, for example, N. A. Scholtus, and W. K. Hall, *J. Chem. Phys.*, **39**, 868 (1963).
(9) F. A. Kuijpers and B. D. Loopstra, *J. Phys. (Paris) Colloq.*, **32**, C1-657 (1971).

Contribution from The Technical University of Denmark, Chemistry Department A, DK-2800 Lyngby, Denmark

Lower Oxidation States of Tellurium. 4. Tetratellurium(2+), Hexatellurium(2+), and Octatellurium(2+) in Chloroaluminate Melts

R. FEHRMANN, N. J. BJERRUM,* and H. A. ANDREASEN

Received January 15, 1976 AIC60040L

The solvated entities Te_4^{2+}, Te_6^{2+}, and Te_8^{2+} have been identified in reaction mixtures of dilute solutions of $TeCl_4$ and elementary tellurium by a combination of a spectrophotometric and a potentiometric method. The spectra of the individual tellurium species in the low-melting NaCl–$AlCl_3$ (37:63 mol %) solvent at 250 °C are calculated from the spectra of the experimental mixtures. pK values (based on molar concentrations) for the reactions $2Te^{4+}(soln) + 7Te_6^{2+}(soln) \rightleftarrows 11Te_4^{2+}(soln)$ and $Te_4^{2+}(soln) + Te_8^{2+}(soln) \rightleftarrows 2Te_6^{2+}(soln)$ were found by both methods. The spectrophotometric method (at 250 °C) gave for the two reactions pK values of −12 and −0.4 with nonlinear confidence limits (95%) of $-\infty$ to −9 and −2.2 to −0.2, respectively. The potentiometric method (at 150 °C) gave for the two reactions pK values of −17 and −0.93 with nonlinear confidence limits (95%) of $-\infty$ to −10 and −1.03 to −0.84, respectively.

Introduction

Previously[1] it has been mentioned that in an NaCl–$AlCl_3$ (37:63 mol %) melt three low oxidation states of tellurium seem to be formed, when Te(IV) is reduced with tellurium. One of these species has been shown[1] to be Te_4^{2+}, whereas the other species have only been suggested to be Te_6^{2+} and Te_8^{2+}.[2] In